AD-A068 768 POLYTECHNIC INST OF NEW YORK FARMINGDALE DEPT OF MEC--ETC F/G 20/4
NAVIER-STOKES CALCULATIONS WITH A COUPLED STRONGLY IMPLICIT MET--ETC(U)
JAN 79 S G RUBIN, P K KHOSLA F49620-78-C-0020

UNCLASSIFIED POLY-M/AE-79-2-PT-1 AFOSR-TR-79-0626 NL

| OF |
AD
A068768

END
DATE
FILMED
7 -79
DDC

SECURITY CLASSIFICATION OF THIS PAGE (When Data Entered)

REPORT DOCUMENTATION PAGE

READ INSTRUCTIONS BEFORE COMPLETING FORM

1. REPORT NUMBER: AFOSR-TR-79-0626	2. GOVT ACCESSION NO.
3. RECIPIENT'S CATALOG NUMBER	
4. TITLE (and Subtitle): NAVIER-STOKES CALCULATIONS WITH A COUPLED STRONGLY IMPLICIT METHOD, PART 1. FINITE-DIFFERENCE SOLUTIONS	5. TYPE OF REPORT & PERIOD COVERED: INTERIM rept.
6. PERFORMING ORG. REPORT NUMBER: Poly-M/AE [illegible]-79-2 Pt-1	
7. AUTHOR(s): STANLEY G. RUBIN, PREM K. KHOSLA	8. CONTRACT OR GRANT NUMBER(s): F49620-78-C-0020
9. PERFORMING ORGANIZATION NAME AND ADDRESS: POLYTECHNIC INSTITUTE OF NEW YORK, AERODYNAMICS LABORATORIES/ ROUTE 110, FARMINGDALE, NY 11735	10. PROGRAM ELEMENT, PROJECT, TASK AREA & WORK UNIT NUMBERS: 2307A1, 61102F, AI
11. CONTROLLING OFFICE NAME AND ADDRESS: AIR FORCE OFFICE OF SCIENTIFIC RESEARCH/NA, BLDG 410, BOLLING AIR FORCE BASE, D C 20332	12. REPORT DATE: Jan 79
	13. NUMBER OF PAGES: 13
14. MONITORING AGENCY NAME & ADDRESS (if different from Controlling Office): 14p.	15. SECURITY CLASS. (of this report): UNCLASSIFIED
	15a. DECLASSIFICATION/DOWNGRADING SCHEDULE

LEVEL II

16. DISTRIBUTION STATEMENT (of this Report)

Approved for public release; distribution unlimited.

17. DISTRIBUTION STATEMENT (of the abstract entered in Block 20, if different from Report)

18. SUPPLEMENTARY NOTES

Aerospace Sciences Meeting, 17th, New Orleans, LA, 15-17 Jan 79

19. KEY WORDS (Continue on reverse side if necessary and identify by block number)

STRONGLY IMPLICIT
VORTICITY-STREAM FUNCTION
COUPLED BOUNDARY CONDITIONS
SECOND-ORDER ACCURATE
CENTRAL DIFFERENCING
LARGE GRID ASPECT RATIOS
STEADY STATE SOLVER
SEPARATED FLOWS

20. ABSTRACT (Continue on reverse side if necessary and identify by block number)

Stone's unconditionally stable, strongly implicit numerical method is extended to the 2x2 coupled vorticity-stream function form of the Navier-stokes equations. The solution algorithm allows for complete coupling of the boundary conditions. Solutions for arbitrary large time steps, and for cell Reynolds numbers much greater than two have been obtained. The method converges quite rapidly without adding artificial viscosity or the necessity for under relaxation. This technique is used here to solve for a variety of internal and external flow problems. Moderate to large Reynolds numbers are considered for both separated and unseparated flows. The procedure is extended to higher-order splines in Part 2 of this study.

DD FORM 1 JAN 73 1473

410 938

UNCLASSIFIED

SECURITY CLASSIFICATION OF THIS PAGE (When Data Entered)

79-0011

Navier-Stokes Calculations with a Coupled Strongly Implicit Method Part 1: Finite-Difference Solutions

S.G. Rubin and P.K. Khosla, *Polytechnic Institute of New York, Farmingdale, N.Y.*

17th AEROSPACE SCIENCES MEETING

New Orleans, La./January 15-17, 1979

NAVIER-STOKES CALCULATIONS WITH A COUPLED STRONGLY IMPLICIT METHOD
PART 1: FINITE-DIFFERENCE SOLUTIONS

S.G. Rubin* and P.K. Khosla**
Aerodynamics Laboratories
Polytechnic Institute of New York
Farmingdale, NY 11735

Abstract

Stone's unconditionally stable, strongly implicit numerical method is extended to the 2x2 coupled vorticity - stream function form of the Navier-Stokes equations. The solution algorithm allows for complete coupling of the boundary conditions. Solutions for arbitrary large time steps, and for cell Reynolds numbers much greater than two have been obtained. The method converges quite rapidly without adding artificial viscosity or the necessity for underrelaxation. This technique is used here to solve for a variety of internal and external flow problems. Moderate to large Reynolds numbers are considered for both separated and unseparated flows. The procedure is extended to higher-order splines in Part 2 of this study.

1. Introduction

A numerical solution procedure for the Navier-Stokes equations in vorticity-stream function form is considered. In the past, almost all explicit and implicit numerical systems that have been developed for these equations have been solved iteratively. It has generally been observed that for stability purposes, a nearly converged solution of the Poisson equation for the stream function is required at each time level before incrementing the vorticity equation one time step. In order to accelerate the rate of convergence to the steady-state, SOR procedures, modified ADI techniques, strongly implicit methods and direct solvers have been considered for the solution of the Poisson equation. For the vorticity transport equation, explicit integration procedures are very time consuming and the temporal increment is restricted by the CFL condition. Implicit methods, though unconditionally stable, usually exhibit spurious oscillations and/or instability for large time steps and/or large cell Reynolds numbers. Moreover, the inversion of the governing tridiagonal system is only assured if the conditions for diagonal dominance (Courant number less than one and cell Reynolds number less than two) are satisfied. The addition of artificial viscosity or the use of upwind differencing (which also contains large amounts of artificial viscosity) usually assures diagonal dominance, but lowers the over-all accuracy or adds excessive numerical diffusion. Furthermore, in many instances, it has been necessary to underrelax in the initial stages of the calculation in order to obtain a converged solution. This is a very time-consuming process.

In the present paper, Stone's strongly implicit method[1] is reformulated to allow for the solution of a 2x2 coupled system of equations. The vorticity-stream function form of the Navier-Stokes equations, with second-order accurate centered differences, is solved by this coupled strongly implicit procedure. The solution algorithm also allows for the coupling of the boundary conditions on the stream function and vorticity in both coordinate directions. Solutions for arbitrary large time steps ($\Delta t \sim 10^{6}$) and cell Reynolds numbers much greater than two are possible. Results have been obtained without adding artificial viscosity and without the necessity of underrelaxation. Even with rather arbitrary initial conditions, the method converges quite rapidly to the steady-state solution, when one exists.

This procedure has been used here to solve for a variety of flow problems at moderately large laminar Reynolds numbers, generally $R_e \leq 2000$. The flow in a driven cavity, the associated temperature field in the cavity, the flow in a channel with a rearward facing step, the flow over a finite length flat plate, and the flow over a circular cylinder will be presented.

In the next section, the solution procedure is described. One of the important limitations of the present technique is the comparatively large storage requirement for the inversion algorithm. However, in the absence of any direct solvers for the nonlinear coupled equations considered here, the ability to obtain converged Navier-Stokes solutions at moderately large Reynolds numbers in modest computer times is particularly attractive. In a second part of this study, higher-order spline collocation procedures are applied with this coupled algorithm. This significantly reduces the grid and therefore the storage requirements.

2. Strongly Implicit Procedure

Finite-difference solutions of partial differential equations of elliptic or parabolic type require the solution of algebraic systems of the following type:

$$A_{ij}W_{i,j-1} + B_{ij}W_{ij} + C_{ij}W_{i,j+1} + D_{i,j}W_{i-1,j} + E_{ij}W_{i+1,j} = G_{ij} \quad (1a)$$

† This research was supported by the Air Force Office of Scientific Research under Contract F-49620-78-C-0020, Project No. 2307-AI

* Professor of Mechanical and Aerospace Engineering, Associate Fellow AIAA
**Associate Professor of Mechanical and Aerospace Engineering, Member AIAA

In matrix form this can be written as

$$\tilde{L}W = G \quad , \tag{1b}$$

where $\tilde{L}$ is a NxN matrix of the following form:

$$\tilde{L} = \begin{bmatrix} C_1D_1 & E_1 & & \\ B_2C_2D_2 & E_2 & \bigcirc & \bigcirc \\ -B_3C_3D_3 & E_3 & & \end{bmatrix} \tag{2}$$

The solution of these equations have been obtained by a variety of techniques, including direct solution by Gaussian elimination or iterative methods such as SOR, ADI, etc.[2] Stone[1] developed a strongly implicit method, which is more rapidly convergent and is based on a quasi-LU decomposition of the matrix $\tilde{L}$.

Direct solvers such as those due to Buneman,[3] Sweet and Schwarztrauber,[4] Bank,[5] etc. are only applicable to a special class of the difference equations (1) and associated boundary conditions. These direct methods are not presently useful for the general finite-difference form of each of the Navier-Stokes equations and certainly not for the coupled vorticity-stream function system. With appropriate boundary conditions the Poisson equation is amenable to direct methods; however, some iterative numerical procedure is required for the uncoupled vorticity equation. Other variants of Gaussian elimination are extremely inefficient and time consuming and even susceptible to a large accumulation of round-off error. SOR and ADI techniques converge rather slowly and for certain types of differencing (involving 9 points) SOR may not converge at all.

Stone's strongly implicit iterative technique falls under the general category of "factorization methods". The underlying idea of factorization is to replace the sparse matrix $\tilde{L}$ by a modified form (L+P) such that the resulting matrix can be decomposed into upper (U) and lower (L) triangular sparse matrices. This leads to the following general iterative procedure for the system (1):

$$(\tilde{L}+P)W^{n+1} = G+PW^n \quad , \tag{3a}$$

or if $\tilde{L}+P = A$, then $AW^{n+1} = G+PW^n$. (3b)

where the superscript n denotes the iteration number. The rate of convergence of this iteration scheme depends upon the particular choice of the matrix P. The two essential requirements on the matrix P are as follows: i) the elements of P should be small in magnitude so that the explicit perturbation is small and ii) the resulting matrix A should be decomposable into sparse L,U factors. If the L and U factors are not sparse, which will be the case if P is a null matrix and L is formed from the finite-difference form of the Navier-Stokes equations, then the usual problems associated with the Gauss elimination procedure can reappear.

There are an infinity of choices of the matrix P for which the LU factors will be sparse. For example, a choice of P such that A becomes a diagonal matrix with the diagonal terms equal to the diagonal of $\tilde{L}$ leads to the familiar point Jacobi iterative procedure.[2] The Gauss-Siedel[2] method is recovered by chosing P such that A is the lower triangular part of the matrix $\tilde{L}$.

Although many other variants are possible, the primary contribution of Stone has been to devise the factorization in such a way that a certain degree of implicitness is associated with each coordinate direction and such that every element in PW^n is small; in particular, the elements are of order h^2, where h is the mesh width. However, Saylor[6] infers that a first-order factorization can be more useful than those that lead to second-order correction terms. In any event, PW^n should tend to zero as h vanishes. An undesirable feature of Stone's factorization is that the matrix P changes at each step so that two successive iterations are in a sense uncorrelated. Although, the ideal factorization may depend upon the particular problem being considered or upon previous experience, the algorithm presented herein is sufficiently general for all types of factorization. The final two-pass algorithm can be written as:

$$(\tilde{L}+P)\ W^{n+1} = AW^{n+1} = G+PW^n \tag{3}$$

$$\tilde{L}V = G+PW^n \quad , \quad UW^{n+1} = \tilde{V} \tag{4a,b}$$

In Stone's factorization procedure P is prescribed such that L and U have only three non-zero diagonals. This leads to a solution of the following form:

$$W_{ij}^{n+1} = \tilde{V}_{ij} + E_{ij}\, W_{i,j+1}^{n+1} + F_{ij}\, W_{i+1,j}^{n+1} \tag{4c}$$

This procedure has the distinct advantage of being implicit in both the i and j directions, as well as coupling all the boundary conditions. We have found that this technique generally converges more rapidly than do many of the more familiar, less implicit, iterative methods previously mentioned. Moreover, it is the present authors' opinion that the lack of implicitness and coupling may explain some of the difficulties that others have encountered in their solutions of high Reynolds number Navier-Stokes flows, in particular, those concerning the CFL limitation, the need for artificial viscosity and the need for underrelaxation. In view of these observations it would appear that a direct solver would be most suitable for the solution of the algebraic system of difference equations (1) arising from the Navier-Stokes equations. Unfortuantely, as noted pre-

viously, currently available efficient direct solvers are not applicable to coupled 2x2 non-linear systems, while others are inefficient, time consuming and suffer from instability due to round-off accumulation. The strongly implicit iterative procedure can provide the necessary coupling of the dependent variables and boundary conditions, and add a significant degree of efficiency and speed of convergence. On the other hand, computer storage requirements are increased. This problem can be minimized by reducing the required number of grid points. With the higher-order methods to be presented in Part 2 this becomes possible.

In the next section, the factorization procedure will be developed for a coupled 2x2 system, e.g., the vorticity-stream function form of the two-dimensional Navier-Stokes equations.

3. Coupled 2x2 Algorithm

Jacobs[7] has extended Stone's algorithm for the second-order accurate nine-point central difference form of the biharmonic operator. He applied the algorithm to the stream function form of the Navier-Stokes equations. The algorithm was used to investigate the flow in a driven cavity. Jacobs could not obtain converged solutions for large Reynolds numbers, i.e., $R_e > 400$. The failure of the algorithm could be associated with the iterative procedure for implementing the boundary conditions. Our own experience with the strongly implicit procedure indicates that the use of iterative boundary conditions considerably reduces the applicability (convergence rate, stability) of the algorithm. Therefore, a 2x2 coupled strongly implicit algorithm has been developed for the stream-function/vorticity form of the Navier-Stokes equation. The finite-difference form of these equations are as follows:

$$A_1\omega_{i,j-1}+B_1\omega_{ij}+C_1\omega_{i,j+1}+D_1\omega_{i-1,j}+E_1\omega_{i+1,j}+$$
$$+A_2\psi_{i,j-1}+B_2\psi_{i,j}+C_2\psi_{i,j+1}+ \qquad (5a)$$
$$+D_2\psi_{i-1,j}+E_2\psi_{i+1,j} = G_1 \ ,$$

and

$$A_3\omega_{i,j-1}+B_3\omega_{ij}+C_3\omega_{i,j+1}+D_3\omega_{i-1,j}+E_3\omega_{i+1,j}+$$
$$+A_4\psi_{i,j-1}+B_4\psi_{ij}+C_4\psi_{i,j+1}+D_4\psi_{i-1,j}+ \qquad (5b)$$
$$+E_4\psi_{i+1,j} = G_2 \ .$$

Direct solution of these equations by variants of Gaussian elimination is very inefficient and expensive. The strongly implicit procedure, though iterative in nature, provides the appropriate coupling and implicitness required for convergence. The factorization procedure given in the preceding section is quite general and is applicable to equations (5a,b) as well.

The iterative solution is given as:

$$[\tilde{L}+\tilde{P}]\,\tilde{W}^{n+1} = \tilde{G} + \tilde{P}\tilde{W}^{n}$$

where $\tilde{W} = \begin{bmatrix} \bar{\omega}_j \\ - \\ \bar{\psi}_j \end{bmatrix}$; $\bar{\omega}_j = \begin{bmatrix} \omega_{1j} \\ \omega_{2j} \\ \cdot \\ \cdot \\ \cdot \\ \omega_{Nj} \end{bmatrix}$;

$$\bar{\psi}_j = \begin{bmatrix} \psi_{1j} \\ \psi_{2j} \\ \cdot \\ \cdot \\ \cdot \\ \psi_{Nj} \end{bmatrix} \qquad G = \begin{bmatrix} G_1 \\ G_2 \end{bmatrix}$$

As described in Section 2, the following two-pass algorithm for equations (5a,b) is obtained:

$$\begin{bmatrix} \omega_{ij} \\ \psi_{ij} \end{bmatrix}^{n+1} = \begin{bmatrix} GM1_{ij} \\ GM2_{ij} \end{bmatrix}^{n} + \begin{bmatrix} T1_{ij} & T3_{ij} \\ T5_{ij} & T7_{ij} \end{bmatrix}^{n} \begin{bmatrix} \omega_{i,j+1} \\ \psi_{i,j+1} \end{bmatrix}^{n+1} \qquad (6)$$
$$+ \begin{bmatrix} T2_{ij} & T4_{ij} \\ T6_{ij} & T8_{ij} \end{bmatrix}^{n} \begin{bmatrix} \omega_{i+1,j} \\ \psi_{i+1,j} \end{bmatrix}^{n+1} ,$$

See the Appendix for the recurrence relationships.

Note that the evaluation of ω_{ij} depends not only upon the other values of ω, but also upon the new values of ψ. The coupling of ω and ψ at the boundaries is exact. In a single iteration, the calculation along arrays close to the boundaries is very close to an exact solution. When the boundary conditions (no-slip conditions) are satisfied iteratively, this feature of the algorithm is lost and the solution converges more slowly. In these iterative procedures, the calculation may even become unstable. It is for these reasons that underrelaxation is sometimes required.

The uncoupled algorithm, equation (4), requires three auxiliary functions; the present 2x2 algorithm requires 10 auxiliary functions. This represents an increase in storage requirements by a factor of more than three. Unfortunately, this is one of the serious drawbacks of the present method. However with the (2x2) coupled method, steady-state calculations, without CFL limitations, artificial viscosity, or underrelaxation, can be performed in relatively few iterations. With a smaller computational field, i.e., a coarse mesh, the storage requirements are reduced. Therefore, higher-order techniques for obtaining steady-state solu-

tions with the present method become very desirable. Higher-order spline 4 solutions of the Navier-Stokes equations with the 2x2 coupled algorithm are presented in Part 2 of the present paper. In earlier studies[8,9] of the spline 4 procedure for the Navier-Stokes equations, a reduction of a factor of sixteen in the number of grid points has been realized in order to obtain accuracy comparable with the second-order central difference solution. This reduces the over-all storage, required for execution of the algorithm, by a factor of 160.

4. Governing Equations

The vorticity-stream function form of the two-dimensional Navier-Stokes equations are considered for a number of internal and external flows. The calculations are carried out in a transformed (x,y) coordinate system using conformal mappings to simplify the computational domain.

$$\frac{1}{J}\frac{\partial \omega}{\partial t} + (u\omega)_x + (v\omega)_y = \frac{1}{R_e}\nabla^2\omega \qquad (7a)$$

$$\nabla^2\psi = \omega/J \qquad (7b)$$

$$\frac{1}{J}\frac{\partial T}{\partial t} + (uT)_x + (vT)_y = \frac{1}{PrR_e}\nabla^2 T \qquad (7c)$$

$$u = \psi_y,\ v = -\psi_x \quad , \qquad (7d)$$

where $R_e = Ua/\nu$; U,a are reference velocity and length; ν is the kinematic viscosity; Pr is the Prandtl number; ω and ψ are the vorticity and stream function; u and v are the velocities along the x and y coordinate directions in the transformed plane; T is the temperature and J is the Jacobian of the transformation.

The mapping

$$Z = Z(\zeta)$$

is considered, where $J = \left|\frac{dz}{d\zeta}\right|^2$ and $Z = x + iy$, $\zeta = \bar{x} + i\bar{y}$. $(\bar{x},\bar{y})$ are the physical coordinates. It should be noted that the velocities (u,v) in the transformed plane are not the physical velocities $(\bar{u},\bar{v})$ in the $(\bar{x},\bar{y})$ directions. The mapping defines the relationship between (u,v) and $(\bar{u},\bar{v})$.

Although the equations (8) are written for unsteady flow, only the steady-state is considered in the present study, therefore very large temporal increments ($\Delta t \sim 10^6$) are prescribed. As noted previously, this is possible with the coupled strongly implicit procedure. The appropriate boundary conditions on the solid surfaces are the no-slip conditions and the Dirichlet condition for the stream function. As described by Roache,[2] the calculations can be very sensitive to the inflow and outflow boundary conditions; in the present paper, derivative boundary conditions have been utilized at these boundaries. These will be detailed for the problems to be considered here.

5. Finite-Difference Discretization

The following difference expressions are prescribed for the derivatives ϕ_x, ϕ_{xx}:

$$\phi_x = \frac{\phi_{i+1}-\phi_{i-1}}{(1+\sigma_1)k_i}\ ;\ k_i = x_i - x_{i-1}\ ,\ \sigma_1 = k_{i+1}/k_i$$

$$\phi_{xx} = \frac{2(\phi_{i+1} - (1+\sigma_1)\phi_i + \sigma_1\phi_{i-1})}{\sigma_1(1+\sigma_1)k_i^2} \quad , \qquad (8)$$

where ϕ is any of the physical variables. A non-uniform grid is prescribed with $\sigma_1 = 1+0(k_i)$ in order to maintain second-order accuracy of the difference formulas. If u and v, in the vorticity transport equation, are treated explicitly, the governing equations are implicitly coupled only through the boundary conditions. In order to strengthen the ψ-ω coupling, the non-linear convective terms will be quasi-linearized. The K-R differencing scheme[10] is applied for the vorticity transport equations. This differencing technique is in effect a splitting of the convective terms into an implicit upwind term and an explicit effective diffusive corrector. Physical diffusion terms are treated implicitly. The converged steady-state solution is second-order accurate. This deferred correction procedure although apparently obvious, has not generally been used and has been found to be of major importance not only in the present context but in the application of higher-order numerical methods. The extension of this scheme to fourth and sixth-order methods, and the associated stability analysis has been presented in reference (9). With the K-R scheme, the convective terms are written as:

$$(u\omega)_x = \mu_x\left[\frac{(u\omega)_{i+1,j} - (u\omega)_{i,j}}{\sigma_1 k_i}\right]^{n+1} + (1-\mu_x)\left[\frac{(u\omega)_{i,j} - (u\omega)_{i-1,j}}{\sigma k_i}\right]^{n+1} + \{1-\mu_x(1+\frac{1}{\sigma_1})\}D^n \quad , \qquad (9a)$$

where D =

$$\frac{(u\omega)_{i+1,j} - (1+\sigma_1)(u\omega)_{ij} + \sigma_1(u\omega)_{i-1,j}}{(1+\sigma_1)k_i} \qquad (9b)$$

and $\mu_x = 0$ if $u_{ij} \geq 0$; $\mu_x = 1$ if $u_{ij} < 0$.

Similar expressions are used for $(v\omega)_y$. The terms $(u\omega)_{ij}$ and $(v\omega_{ij})$ are quasi-linearized to provide the necessary 5-point coupling between ψ and ω during the iterative procedure. It should be noted that there are various other methods for achieving this coupling, e.g., by adding and subtracting the upwind differencing terms at the n+1 and n time levels, respectively. The final converged solution

for (7a,b) is independent of the coupling procedure and the rates of convergence were not noticeably different for the problems considered here. The ideal splitting for the convective terms may depend upon the method of solution of the algebraic system and should provide the maximum rate of convergence. The energy equation (7c) is solved uncoupled from the (ψ,ω) system once the u,v values have been obtained.

6. Boundary Conditions

The boundary conditions on ψ and ω for the strongly implicit procedure are satisfied in the same manner as for the simple one-dimensional LU decomposition or as it is sometimes termed the Thomas algorithm.[2] The distinct advantage of the present coupled procedure is that all the boundaries interact implicitly and simultaneously. For example, if we consider the no-slip condition at a solid surface, the usual first-order boundary condition for (ψ,ω) is

$$\omega_{i,1} = \frac{2J}{h_2^2}\,(\psi_{i,2} - \psi_{i,1}) \qquad (10)$$

In an uncoupled procedure, the wall vorticity is updated after ψ has been evaluated everywhere. In the present coupled procedure, equation (10) is satisfied exactly in each iteration. In order to fully utilize the positive features of the algorithm, it is highly desirable that all the boundary conditions are coupled implicitly. The second-order no-slip condition (11) is used for all of the present calculations

$$\omega_{i,1}^{n+1} = \frac{2J}{h_2^2}\left\{\psi_{i,2}-\psi_{i,1}\right\}^{n+1} - \frac{2J}{\sigma_2(1+\sigma_2)(2+\sigma_2)h_2^2}\left[\psi_{i,3}-(1+\sigma_2)\psi_{i,2}+\sigma_2\psi_{i,1}\right]^{n} \qquad (11)$$

where $\sigma_2 = h_3/h_2$

The bracketed portion is treated implicitly. The correction term enters explicitly. The deferred approach for the higher-order correction to the boundary condition has also been applied for the central difference corrector to upwind differencing in what is termed the K-R procedure[10] and for higher-order splines in Part 2 of the present analysis, see reference (9).

7. Examples

7.1 Cavity Flow

The flow in a driven cavity, see Fig. 1, has been investigated by many authors using a variety of iterative procedures, e.g., see references (11-13). Burggraf[12] in one of the first analyses obtained solutions for $R_e < 400$ with the SOR method and the steady state form of the $(\psi-\omega)$ equations. Underrelaxation was required in the

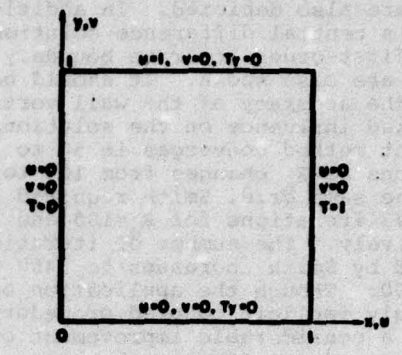

FIG. 1 CAVITY GEOMETRY AND BOUNDARY CONDITIONS

initial stages of the calcuation. A converged solution for the stream function is obtained and then the vorticity is updated in the time iteration. Many iterative studies have followed; more recently, Buneman's direct solver for ψ and the hopscotch or ADI methods for the conservation form of the vorticity transport equation were employed successfully by Smith.[13] He has been able to obtain central difference solutions for $R_e < 5000$. This procedure requires a small Δt (though not limited by the CFL-condition) for stability and consequently takes a longer time for convergence to the steady state. Nallasamy et al.[14] applied upwind differencing to obtain solutions for $R_e < 50{,}000$. This procedure however suffers from large numerical viscosity and therefore the effective R_e is in fact very low. The application of the strongly implicit method for the biharmonic stream function form of the Navier-Stokes equations was considered by Jacobs.[7] As previously noted, these calculations diverged for $R_e \geq 400$.

In the present paper, solutions for $R_e < 3000$ have been obtained with $\Delta t = 10^{-6}$, a 17x17 grid, and with the strongly implicit coupled procedure outlined previously. Arbitrary initial conditions were assumed. The results obtained here are identical to those found previously by direct solver, SOR or ADI methods, when such solutions were possible. The velocity distribution through the vortex center for R_e=1000 and 2000 is shown in Fig. 2, the values of

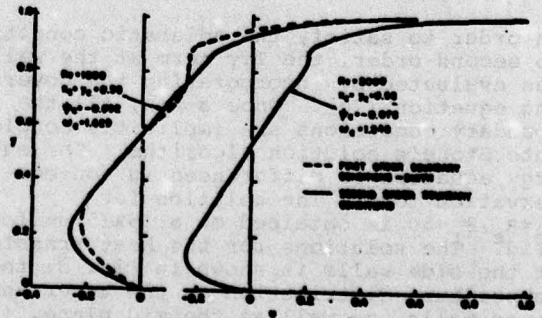

FIG. 2 VELOCITY PROFILES THROUGH VORTEX CENTER CAVITY

maximum stream function, position of the vortex center and the value of the vorticity are also depicted. In addition, Smith's central difference solution, but with first-order accurate boundary conditions are also shown. It should be noted that the accuracy of the wall vorticity has a marked influence on the solution. The present method converges in 50 to 100 iterations as R_e changes from 100 to 3000. For the same grid, Smith required about 120 and 693 iterations for R_e=100 and 1000, respectively. The number of iterations required by Smith increases to 3469 for R_e=5000. Though the application of the strongly implicit coupled procedure represents a considerable improvement over the time dependent methods, the rate of convergence associated with the present zeroth-order factorization procedure can still be improved. Various methods for increasing the rate of convergence will be examined in a future study.

Summarizing our conclusions for the cavity problem, the time dependent methods require large numbers of iterations even with a direct solver for the stream function. Upwind differencing results must be interpreted with caution due to the presence of large amounts of artificial viscosity. In certain cases, as will be shown for the flow over a circular cylinder, upwind differencing can lead to completely incorrect conclusions. The present coupled method, though reasonably fast does require considerably more computer storage than the other techniques for large numbers of grid points. This problem decreases with the higher-order spline methods to be presented in Part 2.

7.2 Heat Transfer in a Driven Cavity

This problem was considered as one of the test cases at the International Conference on Numerical Methods in Laminar and Turbulent Flows held at University College of Swansea.[15] The (u,v) velocity distribution was prescribed. The origin of these profiles is unknown.

The thermal boundary conditions are shown in Fig. 1. The adiabatic wall boundary condition is satisfied by a Taylor series expansion of the form:

$$T_{i,2}=T_{i,1}+h(Ty)_{i,1}+\frac{h^2}{2}(Tyy)_{i,1}+0(h^3). \quad (12)$$

In order to satisfy the adiabatic condition to second-order, the Tyy term at the wall was evaluated by incorporating the governing equation (7c). Once again, all the boundary conditions are implicitly coupled into Stone's solution algorithm. The energy equation is differenced in non-conservation form. The solution for $P_e=R_e \cdot P_r=50$ is obtained on a 15x15 uniform grid. The solutions for the heat transfer at the side walls is shown in Fig. 3; the temperature distribution on the upper and lower walls, as well as the mid plane, is shown in Fig. 4. It should be noted that

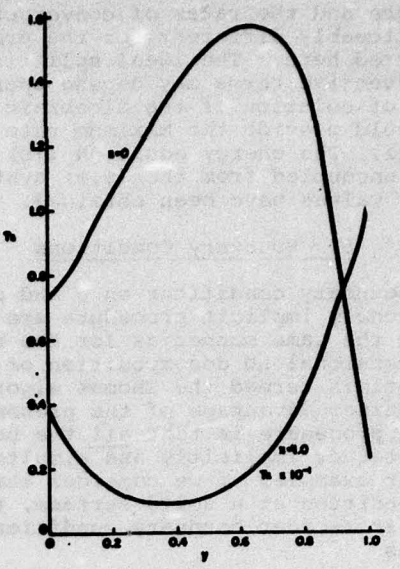

FIG. 3 HEAT TRANSFER ON SIDE WALLS OF CAVITY

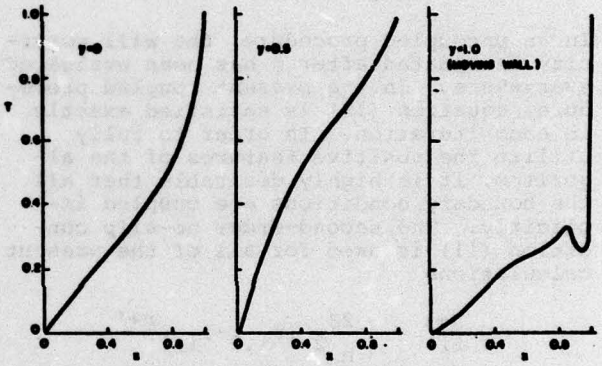

FIG. 4 TEMPERATURE PROFILES IN CAVITY.

the prescribed velocity distribution does not exactly satisfy the continuity equation as applied herein. Therefore, the present results are only as good as the accuracy of these velocity conditions.

7.3 Flow in a Channel with a Backward Facing Step:

The Navier-Stokes equations in primitive variables have been solved by Taylor and Ndefo[16] for the step geometry. Solutions for R_e=25, 100 were obtained using explicit techniques. Recently Roache[11] has investigated the (ψ-ω) equations for this problem. Steady state equations were considered; however, underrelaxation was required to stabilize the solution for the vorticity transport equation. Also, this method of solution is restricted to large grid aspect ratio.

In the present study, the 2x2 coupled algorithm has been used to solve the ψ-ω equations for the step channel. Steady state ($\Delta t=10^6$) solutions for R_e=1, 100 and 1000 have been obtained. The reference

length a in R_e is the channel width k. U is the mean inflow velocity. The step geometry, shown in Fig. 5 is first trans-

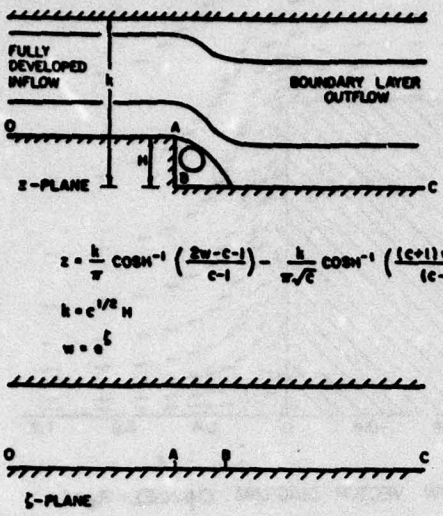

FIG. 5 STEP GEOMETRY IN PHYSICAL AND COMPUTATIONAL PLANES

formed into a straight channel by using the following conformal transformation:[17]

$$z=\frac{k}{\pi}\cos\ h^{-1}\left(\frac{2w-c-1}{c-1}\right)-\frac{k}{\pi\sqrt{c}}\cos\ h^{-1}\left(\frac{(c+1)w-2c}{(c-1)w}\right), \quad (13)$$

$$\zeta = \log w. \quad , \quad k = Hc^{1/2}$$

where H is the step height and k the width of the channel. A 48x21 variable grid, see Fig. 6, is employed in the ζ plane. The mesh aspect ratio varies from a very small number (0.03) to a large number (5810). The convergence of the solution procedure was not sensitive to these large changes in the grid aspect ratio. At the inflow, fully developed conditions are assumed. These conditions are assumed in order to avoid the effect of the entrance boundary layers on the recirculating flow region behind the step. At the outflow, the boundary layer equations are used implicitly as a part of the coupled algorithm. Fully developed flow conditions, which change discontinuously at the step were assumed for the initial guess. It should be pointed out that underrelaxation or artificial viscosity were not required for convergence. For the various Reynolds numbers considered here, convergence was achieved in from 40 to 80 iterations; this compares with 2000 required by Taylor and Ndejo.[16]

In the present calculations, a Reynolds number scaling along the channel was not imposed, to provide optimal resolution in the recirculation bubble. The region of separated flow increases with Reynolds number and this is evident from the present results. The distribution of vorticity along the upper and lower walls is shown in Figs. 7,8 for R_e=1, 100, 1000. The vorticity near the step is shown on an expanded scale in Fig. 8. Vector plots of

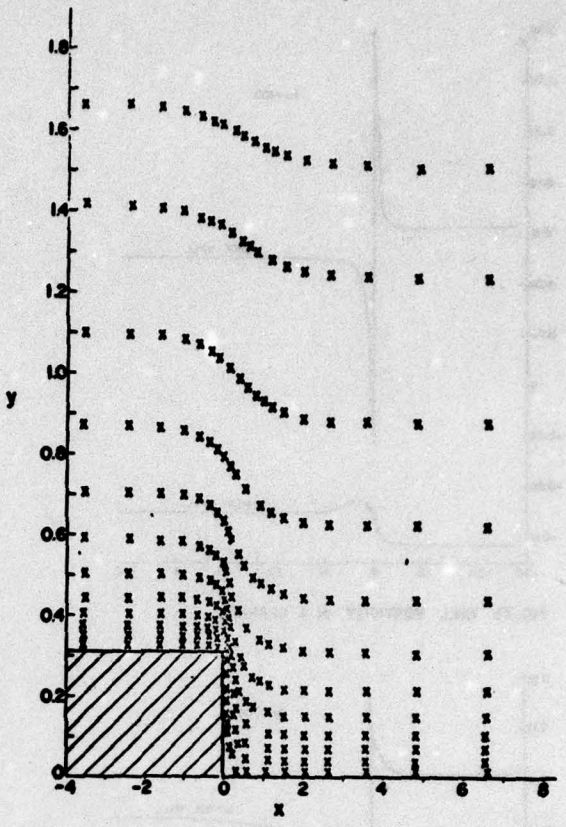

FIG.6 GRID DISTRIBUTION FOR CHANNEL

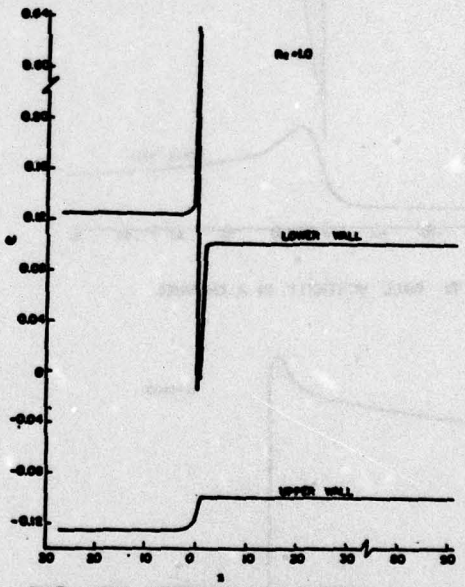

FIG.7a WALL VORTICITY IN A CHANNEL

the streamlines are shown in Fig. 9. It can be seen that for R_e=1, the flow separates below the corner. As the Reynolds number increases, the separation point moves upward toward the corner. Since the transformation (13) is singular at the corner, a grid point was not located at the juncture itself; however, from the calcuated results, the indications are

FIG. 7b WALL VORTICITY IN A CHANNEL

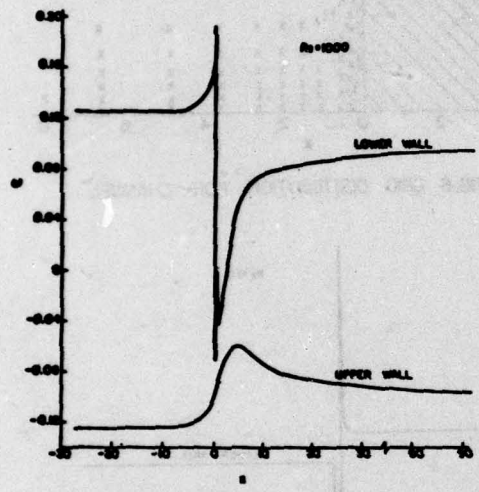

FIG. 7c WALL VORTICITY IN A CHANNEL

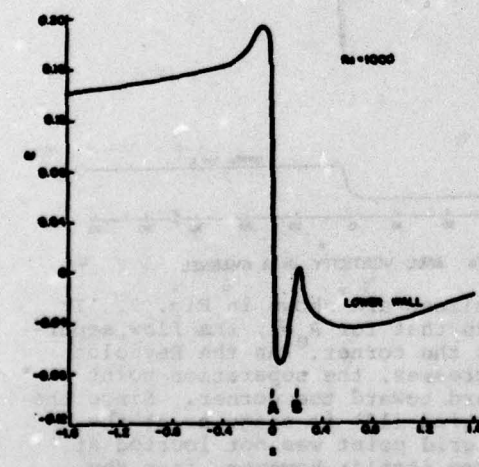

FIG. 8 CHANNEL VORTICITY NEAR STEP

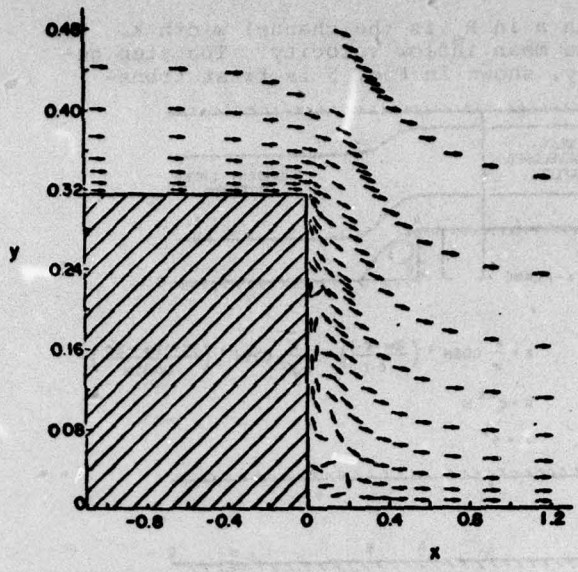

FIG. 9a FLOW VECTOR DIAGRAM: CHANNEL - R_e = 1

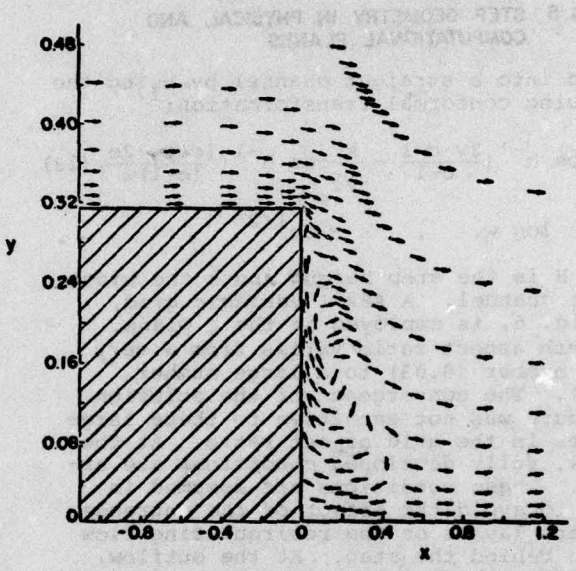

FIG. 9b FLOW VECTOR DIAGRAM: CHANNEL - R_e = 100

that for larger Reynolds numbers the separation point moves even closer to the corner. Although the inflow profiles are independent of the Reynolds number, the flow approaching the corner acquires the characteristics typical of a high R_e boundary layer. The degree of upstream influence is an inverse function of the Reynolds number.

7.4 Flow Over a Flat Plate

Both semi-infinite and finite flat plate flows for unit Reynolds numbers up to 10^5 have been obtained with the 2x2 coupled algorithm. Step initial condition were assumed. These were applied at the leading edge for the semi-infinite plate so that no upstream influence was allowed. This leads to velocity overshoots near the inflow which slowly decay downstream. On the same grid

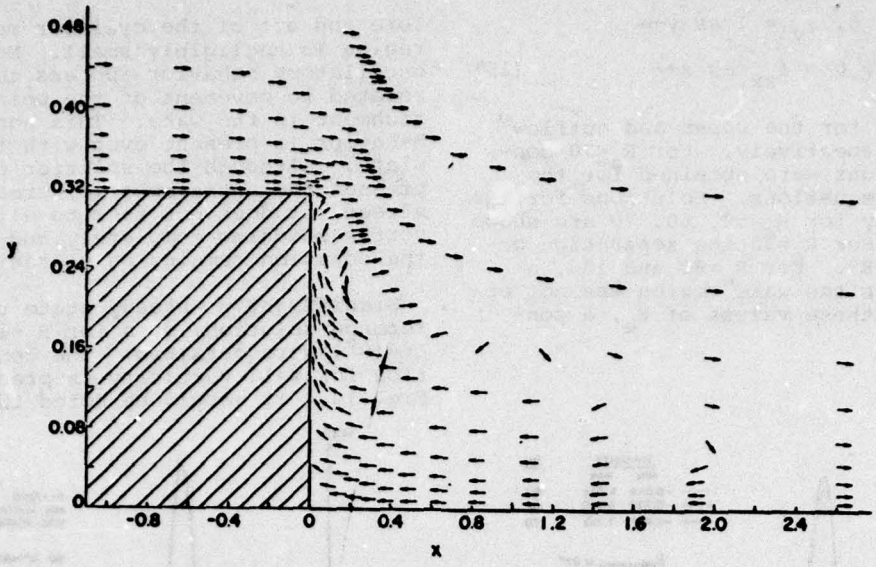

FIG. 9c FLOW VECTOR DIAGRAM: CHANNEL - R_e=1000

a solution of the ψ-ω form of the boundary-layer equations was also obtained. The two results compared very closely. Therefore the relative accuracy and consistency of the central-difference schemes for the Navier-Stokes equation and very large R_e has been demonstrated. If a boundary-layer solution is used at the inflow instead of the step conditions, the overshoots in velocity disappear. Calculations for the finite flat plate with uniform flow far upstream of the leading edge were also convergent and acceptable.

7.5 Flow Over a Circular Cylinder with a Splitter Plate.

The numerical evaluation of the flow over a circular cylinder has been the subject of investigation of many authors.[18] Thom,[19] Kawaguti,[20] Takami and Keller,[21] and Dennis and Chang[22] have considered the steady state equations for (ψ,ω). The resulting second-order central difference equations were solved by SOR or line-relaxation techniques. Except for the work of Dennis and Chang,[22] who obtained solutions for R_e=100, these steady-state calculations have been limited to R_e<60. The reference length in R_e is the cylinder diameter.

The preponderance of studies have used time-dependent methods to evaluate the transient and asymptotic steady state behavior. For large R_e flows, the solution for the wake region is apparently oscillatory and the question of the existence of a steady state solution remains open. Almost all time-dependent calculations suggest that these wake flow oscillations appear for $R_e \geq 100$. Recently, Lin et. al.[22] reinvestigated the cylinder flow with the strongly implicit method. The ψ-ω equations were solved iteratively using Stone's algorithm described herein. Oscillatory wake flow was observed for $R_e > 80$. This contrasts with the "steady-state" solution described by Dennis and Chang for R_e=100. The question of a steady-state limit appears to remain unresolved.

In the present study the coupled 2x2 algorithm is used to reexamine the existence of steady flow solutions. The cylinder with a splitter plate is mapped into a semi-infinite flat plate with the Joukowski transformation, see Fig. 10.

$$\zeta = \frac{1}{2}\left(Z + \frac{1}{Z}\right) \qquad (14)$$

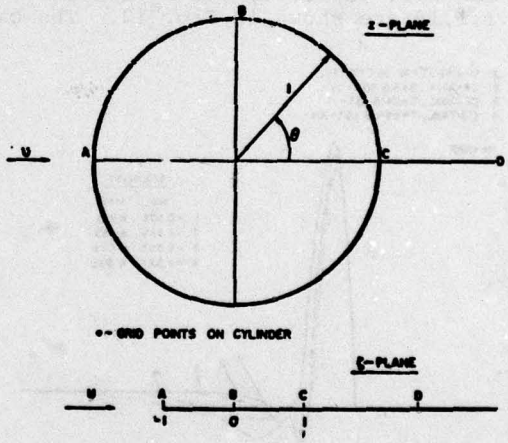

FIG. 10 CYLINDER GEOMETRY

Only the upper half of the flow was considered. A 33x17 variable grid generated from an analytical transformation was prescribed. This grid is very coarse, but adequte for the present purposes. The mesh width at the surface is $(\Delta y) \sim .25$. Fifteen of the 33 points in the axial direction are on the surface of the cylinder, see Fig. 10. Derivative boundary conditions

$$\omega_y = 0,\ \psi_y = 1 \text{ as } y \to \infty$$

$$\omega_{xx} = 0 = \psi_{xx} \text{ as } x \to \infty \qquad (15)$$

were employed for the upper and outflow boundaries respectively. For $R_e \leq 70$ converged solutions were obtained for the steady state equations. Solutions for the wall vorticity for R_e=50, 60, 70 are shown in Fig. 11. For R_e=70 the separation occurs at θ=61.8°. For R_e=80 and 100, a steady flow in the wake region was not obtained. For these values of R_e, a converged steady state solution for the upwind difference equations was obtained. The second-order correction, using the unconditionally stable K-R scheme did not converge for $\Delta t = 10^6$. Solutions were found for smaller values of Δt. The solutions for the wall vorticity for R_e=100 and Δt=.1,1,10 are shown in Fig. 12. The calculations for this problem were carried out on PDP 11/60 in an interactive mode. The solution was monitored at each time step. Even larger values of Δt(=100) were used without any difficulty. The solution however never acquired a steady-state value. As seen from Fig. 12, although the vorticity in the wake changes considerably, the effect on the solution fore and aft of the cylinder recirculation region is negligibly small. Moreover, the oscillatory behavior appears to be closely related to movement of the point of reattachment in the wake. This non-stationary behavior is present even with the splitter plate. Although the splitter plate suppresses the antisymmetric Karman vortex street, it does not seem to eliminate the vortex shedding completely and therefore the solution remains only quasi-steady.

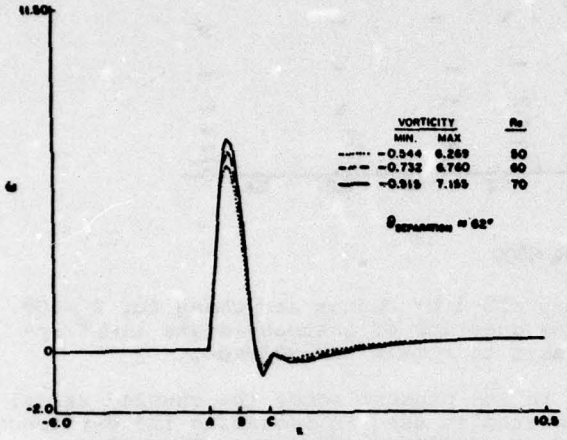

FIG. 11 VORTICITY ALONG SURFACE OF CYLINDER

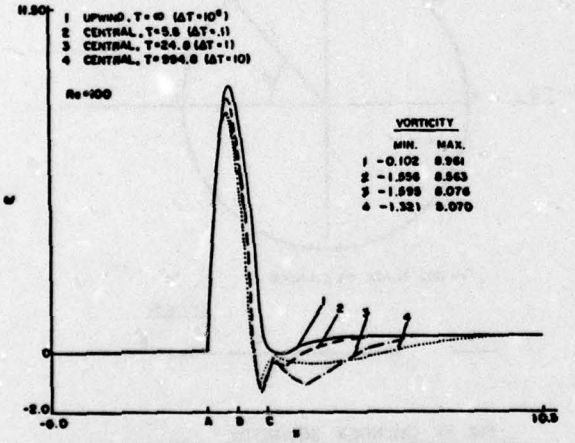

FIG. 12 CYLINDER SURFACE VORTICITY VARIATION WITH TIME, Re=100

Significantly, steady state upwind difference solution, even for R_e=1000 and $\Delta t = 10^6$, were obtained. The converged solution for wall vorticity is presented in Fig. 13. It should be noted that the presence of large amounts of artificial viscosity for the very crude grid considered here reduces the size of the separated flow region suggesting a much smaller effective R_e. This allows for a steady state solution, for a flow which in fact is oscillatory. In the light of this result and others found for the cavity flow, upwind difference results must be viewed with great caution, and in the opinion of the present authors may not be meaningful unless the mesh size is rather small.

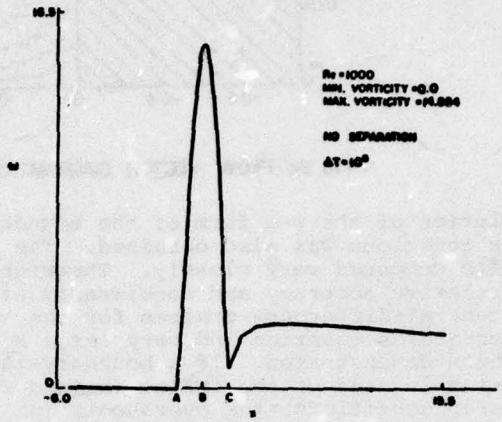

FIG. 13 VORTICITY ALONG CYLINDER SURFACE WITH UPWIND DIFFERENCING

8. Summary

The incompressible vorticity-stream function system of the Navier-Stokes equations has been solved numerically for a variety of flow configurations: (i) driven cavity, (ii) thermal cavity, (iii) channel with a step, (iv) flat plate, (v) circular cylinder with a splitter plate. The important features of the present analysis are as follows: 1) The coupled (ω-ψ) equations, with coupled boundary conditions, are considered. 2) A strongly implicit procedure is applied. 3) The combination of 1) and 2) allows for solutions at relatively large laminar Reynolds numbers ($R_e \leq 3{,}000$); flows with separation regions are included. 4) The time step can be taken arbitrarily large so that in effect this is a steady-state solver. Convergence is achieved in 30 to 100 iterations. 5) Large spatial grids are allowable so that cell Reynolds

numbers are considerably in excess of two. 6) No artificial viscosity is required to obtain second-order accurate central-difference solutions. 7) For the cylinder geometry, steady solutions were found only for R_e<80. For larger Reynolds numbers, transient calculations for smaller time steps depict an oscillatory behavior, that is essentially confined to separation region. 8) It has been demonstrated that strongly implicit solutions are possible for all R_e examined with upwind differencing. This is a result of the large numerical viscosity, which lowers the effective R_e significantly.

References

1. Stone, H.L.: "Iterative Solution of Implicit Approximations of Multidimensional Partial Equations". SIAM J. Numer. Anal., Vol. 5, pp. 530-558 (1968).
2. Roache, P.J.: "Computational Fluid Dynamics". Hermosa Publishers (1972).
3. Buneman, O.: "A Compact Non-iterative Poisson Solver". SUIPR Report 294 Inst. for Plasma Research, Stanford Univ. Calif. (1969).
4. Schwarztrauber, P.N. and Sweet, R.A.: "The Direct Solution of the Discrete Poisson Equation on a Disc". SIAM J. Numer. Anal., Vol. 10, pp. 900-907 (1973).
5. Bank, R.E.: "Marching Algorithms for Elliptic Boundary Value Problems. II: The Variable Coefficient Case:. SIAM J. Numer. Anal., Vol. 5, pp. 950-970 (1977).
6. Saylor, P.: "Second Order Strongly Implicit Symmetric Factorization Methods for the Solution of Elliptic Difference Equations:. SIAM J. Numer. Anal., Vol. 11, pp. 894-908 (1974).
7. Jacobs, D.A.H.: "The Strongly Implicit procedure for Biharmonic Problems". J. of Comput. Physics, Vol. 13, pp. 303-315 (1973).
8. Rubin, S.G. and Khosla, P.K.: "Polynomial Interpolation Methods for Viscous Flow Calculations". J. Comput. Physics. Vol. 24, pp. 217-244 (1977).
9. Rubin, S.G. and Khosla, P.K.: "A Simplified Spline Solution Procedure". Proc. of 6th International Conference on Numerical Methods in Fluid Dynamics held in Tbilisi, USSR. (1978).
10. Khosla, P.K. and Rubin, S.G.: "A Diagonally Dominant Second-Order Accurate Implicit Scheme". Computers and Fluids, Vol. 2, pp. 207-209 (1974).
11. Proc. of 1st International Conf. Numerical Methods in Laminar and Turbulent Flows held at University College Swansea, pp. 873-883 (1978).
12. Burggraf, O.R.: "Analytical and Numerical Studies of Steady Separated Flows". J. Fluid Mech., Vol. 24, pp. 113-151 (1966).
13. Smith, R.E. and Kidd, Amy: "Comparative Study of Two Numerical Techniques for the Solution of Viscous Flow in a Driven Cavity". NASA SP-378 (1975).
14. Nallasmy, M. and Krishna, Prasad, K.: "On Cavity Flow at High Reynolds Numbers". J. Fluid Mech., Vol. 79, pp. 391-414 (1977).
15. Special Session at the International Conf. on Numerical Methods in Laminar and Turbulent Flows held at Univ. College Swansea. Proc. to be published.
16. Taylor, T.D. and Ndefo, E.: "Computation of Viscous Flow in a Channel by the Method of Splitting". Proc. of Second International Conf. on Numerical Methods in Fluid Dynamics, Springer-Verlog Publisher, pp. 356-364 (1970).
17. Kober, H.: "Dictionary of Conformal Representations". Dover Publications, pp. 161 (1957).
18. Thom, A.: "The Flow Past Circular Cylinders at Low Speeds". Proc. Roy. Soc. A141, pp. 651-666 (1933).
19. Kawaguti, M.: "Numerical Solution of the Navier-Stokes Equations for the Flow Around a Circular Cylinder at Reynolds Number 40". J. Phys. Soc. Japan, Vol. 8, pp. 747-757 (1953).
20. Takami, H. and Keller, H.B.: "Steady Two Dimensional Viscous Flow of an Imcompressible Fluid Past a Circular Cylinder"/ Phys. Fluids Supplement II, Vol. 12, pp. 51-56 (1969).
21. Dennis, S.C.R. and Chang, G.Z.: "Numerical Solutions for Steady Flow Past a Circular Cylinder at Reynolds Numbers up to 100". J. Fluid Mech., Vol. 42, pp. 471-489 (1970).
22. Lin, C.L., Pepper, D.W. and Lee, S.C.: "Numerical Methods for Separated Flow Solutions Around a Circular Cylinder". Proc. AIAA Second Computational Fluid Dynamics Conf. Hartford, Connecticut, pp. 91-100 (1975).

Appendix

Recurrence Relationship for 2x2 System:

$$G_{21} = - D_1T_1(i-1,j)-D_2T_5(i-1,j)$$

$$G_{41} = - D_1T_3(i-1,j)-D_2T_7(i-1,j)$$

$$G_{11} = - A_1T_2(i,j-1)-A_2T_6(i,j-1)$$

$$G_{31} = - A_1T_4(i,j-1)-A_2T_8(i,j-1)$$

$$S_{11} = \omega_{i+1,j-1},\ S_{21} = \omega_{i-1,j+1}$$

$$SG_1 = G_1+G_{11}S_{11}+G_{21}S_{21}+G_{31}S_{31}+G_{41}S_{41}$$

$$SG_2 = G_2+G_{12}S_{11}+G_{22}S_{21}+G_{32}S_{31}+G_{42}S_{41}$$

$$GG_2 = SG_2-A_3GM_1(i,j-1)-D_3GM_1(i-1,j) -A_4GM_2(i,j-1)-D_4GM_2(i-1,j)$$

$$Z_2 = B_2+A_1T_3(i,j-1)+D_1T_4(i-1,j) + A_2T_7(i,j-1)+D_2T_8(i-1,j)$$

$$Z_4 = B_4+A_3T_3(i,j-1)+D_3T_4(i-1,j) + A_4T_7(i,j-1)+D_4T_8(i-1,j)$$

$$GM_1(i,j) = (Z_4GG_1-Z_2GG_2)/DM$$

$$T_1(i,j) = (Z_2C_3-Z_4C_1)/DM$$

$$T_3(i,j) = (Z_2C_4-Z_4C2)/DM$$

$$T_5(i,j) = (Z_3C_1-Z_1C_3)/DM$$

$$T_7(i,j) = (Z_3C_2-Z_1C_4)/DM$$

$$G_{22} = - D_3T_1(i-1,j)-D_4T_5(i-1,j)$$

$$G_{42} = - D_3T_3(i-1,j)-D_4T_7(i-1,j)$$

$$G_{12} = - A_3T_2(i,j-1)-A_4T_6(i,j-1)$$

$$G_{32} = - A_3T_4(i,j-1)-A_4T_8(i,j-1)$$

$$S_{31} = \psi_{i+1,j-1},\ S_{41} = \psi_{i-1,j+1}$$

$$GG_1 = SG_1-A_1GM_1(i,j-1)-D_1GM_1(i-1,j) -A_2GM_2(i,j-1)-D_2GM_2(i-1,j)$$

$$Z_1 = B_1+A_1T_1(i,j-1)+D_1T_2(i-1,j) + A_2T_5(i,j-1)+D_2T_6(i-1,j)$$

$$Z_3 = B_3+A_3T_1(i,j-1)+D_3T_2(i-1,j) + A_4T_5(i,j-1)+D_4T_6(i-1,j)$$

$$DM = Z_1Z_4-Z_2Z_3$$

$$GM_2(i,j) = (Z_1GG_2-Z_3GG_1)/DM$$

$$T_2(i,j) = (Z_2E_3-Z_4E_1)/DM$$

$$T_4(i,j) = (Z_2E_4-Z_4E_2)/DM$$

$$T_6(i,j) = (Z_3E_1-Z_1E_3)/DM$$

$$T_8(i,j) = (Z_3E_2-Z_1E_4)/DM$$